Cellulose (2015) 22:2391–2407
DOI 10.1007/s10570-015-0673-4

ORIGINAL PAPER

Study of chitosans interaction with Cu(II) from the corresponding sulfate and chloride salts

Fernanda Stuani Pereira · Glenda Gonçalves de Souza · Paula G. P. Moraes · Rafael Pianca Barroso · Silvania Lanfredi · Homero Marques Gomes · Antonio José Costa-Filho · Eduardo René Pérez González

Received: 18 February 2015 / Accepted: 28 May 2015 / Published online: 4 June 2015

Abstract The interaction of copper ions with chitosan and three synthesized derivatives with different chelating centers, *N*-benzylidene chitosan, *N*-benzyl chitosan and poly-*N*-(4-(4-*R*-methoxyphenyl)diazenyl)-benzyl-chitosan using $CuSO_4{\cdot}5H_2O$ and $CuCl_2{\cdot}2H_2O$ salts was studied. The content of Cu^{2+} in the complexes was determined by atomic absorption spectrometry and the results showed that chitosan exhibited higher chelating capacity for both salts. Morphological changes of derivatives and complexes were demonstrated by SEM–EDS. In addition, the presence of some crystals attributed to copper sulfate adsorbed on the polymer surface was also observed, which indicates that part of the metal content is in the salt adsorbed and might influence in the use of the materials for further application studies. This result was supported by Raman spectroscopy results in which vibrations of O=S=O groups were observed. X-ray diffraction patterns showed that the chemical modification of chitosan and formation of complexes resulted in the decrease of crystallinity. Electron paramagnetic resonance was used to investigate structural aspects of the materials complexed with Cu^{2+} ions in the solid state.

Keywords Chitosan · Derivatives · Copper · Complexes

F. S. Pereira · E. R. P. González (✉)
Laboratório de Química Orgânica Fina, Departamento de Física, Química e Biologia, Univ Estadual Paulista, Campus de Presidente Prudente, C.P. 467, Presidente Prudente, SP 19060-900, Brazil
e-mail: eperez@fct.unesp.br

G. G. de Souza · P. G. P. Moraes · S. Lanfredi · H. M. Gomes
Departamento de Física, Química e Biologia, Univ Estadual Paulista, Campus de Presidente Prudente, C.P. 467, Presidente Prudente, SP 19060-900, Brazil

R. P. Barroso · A. J. Costa-Filho
Laboratório de Biofísica Molecular, Departamento de Física, Faculdade de Filosofia Ciências e Letras de Ribeirão Preto, Universidade de São Paulo, Ribeirão Prêto, SP, Brazil

Introduction

In recent years, chitosan has become a very attractive biopolymer due to its physicochemical and biological properties, such as biocompatibility, biodegradability and non-toxicity. For this reason, chitosan and its derivatives have been explored for different uses in several fields. The –OH and $–NH_2$ groups on the skeleton of chitosan can bind transition metal ions either by chelation or by physical adsorption to form complexes. Thus, chitosan has demonstrated greater chelating ability than chitin.

Copper complexes were found to be important materials in medicinal procedures as they have shown potential use as antimicrobial, antiviral, anti-inflammatory and antitumor agents (Giovagnini et al. 2008; Dulcevscaia et al. 2013; Facchin et al. 2009; Urquiola et al. 2008; Torre et al. 2005) and enzyme inhibitors

(Iakovidis et al. 2011). The chelation of copper ions with chitosan has received considerable attention due to its applications in waste water treatment (Domard 1987; Huang et al. 1996; Bassi et al. 2000), food industries and as catalysts in a variety of reaction systems (Guibal 2005; Calo et al. 2004; Adlim et al. 2004; Wang et al. 2005). Chitosan Cu^{2+} complexes have also been reported for their antibacterial and antitumor properties (Zheng et al. 2006). Results indicated that the inhibitory effects of chitosan–metal complexes can depend on the property of metal ions, the molecular weight and degree of deacetylation of the polymer and environmental pH values (Wang et al. 2005).

Some works have given attention to understand more about the structure of chitosan copper ions. X-ray studies of chitosan transition metal complexes demonstrated that a metal salt is coordinated with an amino group of a dimer residue of chitosan by a "pendant model" (Ogawa and Oka 1993; Ogawa et al. 1984). In agreement with this result, Schlick (1986) reported that ESR parameters suggest that chitosan is bonded through four nitrogen ligands to Cu^{2+} ions in a square-planar geometry (Schlick 1986). Other ESR studies showed that copper ions are trapped in a great amount when the polymer exhibits a lower crystallinity index and a higher deacetylation degree increases the retention capacity (Valdés and Triviño 2009). Cárdenas et al. (2003) reported that EDX studies revealed the highest retention of copper metal ions by chitosan of 1.2×10^{-3} eq/g, which is in agreement with the electron micrograph that exhibit a smooth surface (Cárdenas et al. 2003).

On the other hand, chemical modification of chitosan can change the polymer properties and demonstrate different interaction capacity with metallic ions (Jiao et al. 2001; Rodrigues et al. 1998. Copper(II) complexes of Schiff-bases, for example, are becoming relevant due to the wide applications in several fields (Genin et al. 2000; Suslick and Reinert 1985; Katwal et al. 2013).

The sorptivity capacity of *N*-(2-carboxyethyl) chitosan was studied using a mixture of the appropriate sulfates of Zn^{2+}, Cu^{2+}, Co^{2+}, Ni^{2+} at pH 4.5. The highest capacity and selectivity for Cu(II) reached the maximum capacity up to 3.7 mmol/g; corresponding to 80 %. It was found that anions of the absorbed solution are involved in the sorption (Dobetti and Delben 1992).

Considering the pH media, the sorption of metal cations can be studied at pH close to neutral (Guibal 2004). Rhazi et al. (2002) have reported that the optimal pH for the fixation of cupric ions by chitosan is in the range of 5–7 (Rhazi et al. 2002). In acidic solutions, the protonation of amine groups gives the polymer the potential for attracting metal anions, such as molybdate, vanadate, chromate and arsenate (Chassary et al. 2004). Sorption studies of carboxymethyl and carboxybutyl chitosans have shown that both amino and carboxylic groups are involved in the metal chelation. However, at low pH media, the binding ability of *N*-carboxymethyl chitosan towards Cu(II) and Pb(II) ions decreased (Delben et al. 1992).

Furthermore, azobenzene chitosan derivatives can be studied as metal chelating materials. Wang et al. reported the synthesis, characterization and application of 4-amino-4′-nitro azobenzene modified cross-linked chitosan for the adsorption of Au(III) and Pd(II) from aqueous samples (Wang et al. 2010) and the adsorption capacity of 3′-nitro-4-amino azobenzene modified chitosan toward Pd(II) and Pt(IV) (Wang et al. 2011).

In the present manuscript, we report the interaction of copper ions from aqueous solutions of two different salts, $CuSO_4 \cdot 5H_2O$ and $CuCl_2 \cdot 2H_2O$, with chitosan and its derivatives *N*-benzylidene chitosan (CTB), *N*-benzyl chitosan (NBC) and poly-(4-(4-methoxyphenyl)diazenyl)-*N*-benzyl chitosan (Azo-NBC). *N*-azobenzyl chitosan derivatives have been previously prepared and characterized by thermal and spectroscopy (Pereira et al. 2013, 2014). The series of chitosan derivatives were employed in this work to study the influence of different chelating centers for Cu(II). The biological activity of complexes can be related to the amount of ions coordinated and the coordination mode of the metal with specific centers, in which can present different crystallinity, bond lengths and bond angles (Haas and Franz 2009). In addition, for the use of metal complexes in catalytic systems, it is of great importance to investigate the most active form of the complex in relation to its coordination center (Das et al. 2014). Another point for studying these materials is their lack of solubility in the majority of common solvents tested, which make them excellent candidates for use as heterogeneous catalysts due to their recovery and reusability (Anastas et al. 2001).

The influence of both salts on the copper complexation reaction was analyzed by AAS and the complexes with higher Cu^{2+} content were characterized by SEM–EDS, XRD, Raman and EPR.

Materials and methods

Materials

Chitosan from crab shells was purchased from Sigma-Aldrich, lot # SLBC2867V and cat # 417963, humidity: 11.8 %, and was used without further purification. The deacetylation degree of chitosan was 78 %. The other chemicals used were of analytical grade. Benzaldehyde, sodium cyanoborohydride, copper(II) sulfate pentahydrate and copper(II) chloride dihydrate were purchased from Sigma-Aldrich and used without further purification.

N-alkylation of chitosan

Chitosan derivatives were prepared according to the literature (Borch et al. 1971). For the preparation of the Schiff-base, 0.5 g of chitosan was dissolved in 15 mL of acetic acid 1 % and the pH was adjusted to 4–5. This solution was diluted with 30 mL of ethanol and stirred for 30 min to form a colorless gel. Then, 2 mmol of benzaldehyde dissolved in 10 mL of ethanol (99 %) was added to the solution and the mixture was stirred for 8 h at 60 °C. After that, the solvent was evaporated under reduced pressure and the product was washed with 15 mL of aqueous $NaHCO_3$ (5 %). The product was filtered off and washed with distilled water and ethanol to remove the excess of reagents. The resulting yellowish powder was dried for 4 h at 60 °C and yielded 0.65 g. The degree of substitution (DS) determined by ^{1}H-NMR (Sajomsang et al. 2006) was 52 %.

The Schiff base was reduced with sodium cyanoborohydride (0.12 g, 2 mmol) dissolved in 10 mL of ethanol (99 %) and the mixture was stirred for 24 h at room temperature. The white precipitate was filtered off and washed with water and ethanol to remove the excess of reagents. Afterwards, the material was dried for 4 h at 60 °C, yielding 0.7 g of product. The DS determined by ^{1}H-NMR (Sajomsang et al. 2006) was 50 %.

Synthesis of the *N*-azobenzyl derivative (Azo-NBC)

1 mmol of *p*-methoxybenzenediazonium tetrafluorborate (0.19 g) was dissolved in 10 mL of acetonitrile. *N*-benzyl chitosan (0.5 g) was slowly added to the solutions and the mixture was stirred for 30 min at 0–5 °C. The dark brown product was filtered off, washed with ethanol and dried for 3 h at 40 °C. The product showed solubility in dimethyl sulfoxide (DMSO). The DS determined by ^{1}H-NMR (Sajomsang et al. 2006) was 46 %.

Preparation of chitosan and derivatives copper complexes

The complexes were prepared by adding 0.1 g of dry chitosan or derivatives (CTB, NBC and Azo-NBC) to 10 mL of $CuSO_4{\cdot}5H_2O$ or $CuCl_2{\cdot}2H_2O$ aqueous solution (0.01 mol/L) with stirring at room temperature. In order to investigate the influence of the reaction time, the formation of metal complex was studied from 30 min to 48 h. After stirring during the corresponding time, the mixture was filtered off and the precipitate was dried in an oven at 60 °C for 4 h. The obtained complexes were denominated Chitosan–Cu, CTB–Cu, NBC–Cu and Azo-NBC–Cu.

Measurements

Cu(II) ions content of the remaining solution was measured by A Model Analyst 200 PerkinElmer Atomic Absorption Spectrometer in the optimal conditions recommended by the supplier for this quantification.

The electron micrograph studies were carried out in Carls Zeiss EVO LS15 Model, with secondary electrons detector and high vacuum. Sputter Coater Quorum Model Q 150R ES was used to metalize the samples.

X-ray diffractograms on powder samples were obtained using a SHIMADZU (model XRD-6000) diffractometer, with Cu-Kα_1 radiation ($\lambda = 1.54056$ Å) and a graphite monochromator, at 40 kV and a current of 30 mA. Measurements were carried out over an angular range of $5° \leq 2\theta \leq 40°$ with a scanning step of 0.02° and a fixed counting time of 10 s. Divergence, scattered and receiving radiation slits were 1°, 1° and 0.2 mm respectively.

The Raman spectra were obtained using a micro-Raman spectrograph Renishaw model inVia, equipped with an electrically cooled CCD camera, with laser lines at 532, 633 or 785 nm, and diffraction grades with 1800 and 1200 L/mm, 1 accumulation, 10 s of acquisition and the laser power was adjusted to best relation signal/noise.

EPR spectra were recorded using a JEOL, Model FA-200 (JEOL Ltd., Tokyo, Japan) at X-band. The EPR spectra were measured at the microwave power of 10 mW and amplitude of modulation 8 mT, 2 scans with the sweep time of 4 min.

Results and discussion

The Schiff base has been synthesized by the condensation reaction of chitosan and benzaldehyde. Subsequently, this compound was reduced with $NaBH_3CN$ to yield *N*-benzyl chitosan. *N*-azobenzyl chitosan derivative was prepared via azo-coupling of *N*-benzyl chitosan and the *p*-methoxybenzenediazonium tetrafluoroborate salt, Scheme 1.

Atomic absorption spectrometry (AAS)

Table 1 shows the Cu^{2+} content, from $CuSO_4{\cdot}5H_2O$ solution, adsorbed by chitosan and derivatives determined by AAS in different reaction times. The results showed that the maximum chelating capacity of chitosan was when the reaction occurred during 24 h. For the derivatives, the higher concentration of copper ions chelated was obtained with 36 h of reaction time. The results also show that chitosan is the most efficient chelating agent, adsorbing 120 mg of Cu(II) ions by gram of polymer, which corresponds to 75 % of adsorption. As the chemical modification occurs in the polymer chain the adsorption capacity decreases, probably due to the decrease of free amino groups, one of the chelating sites. Another reason might be the steric hindrance of the new groups bonded to chitosan. Therefore, for chitosan derivatives, Cu^{2+} ions might be coordinated by the amino groups which are not chemically modified. The best results are shown in bold in Table 1.

The pH of Cu^{2+} solutions before the complexation reaction was 6.5, as the optimum pH range reported by Rhazi et al. (2002). After the reaction time, the pH was measured and the obtained value was 5.2 for all compounds. The formation of the complexes may be accompanied by the release of a proton for the coordination, and consequently, the decrease of the pH (Rhazi et al. 2002).

The formation of chitosan and derivatives Cu(II) complexes was also investigated using $CuCl_2{\cdot}2H_2O$ salt as the precursor of copper ions. The reactions were carried out at the time previously determined, 24 h for chitosan and 36 h for the derivatives. The chelation capacities of these materials were studied by AAS and are listed in Table 2. The copper content chelated by the compounds using $CuCl_2{\cdot}2H_2O$ salt is lower when compared to the results observed for the reaction with $CuSO_4{\cdot}5H_2O$. However, part of the copper amount present in the polymeric compounds is in the form of copper sulfate salt adsorbed on the surface of chitosan and derivatives, as evidenced by SEM–EDS analysis. On the other hand, no $CuCl_2{\cdot}2H_2O$ salt was observed on the polymeric surface, therefore, the complexation reaction with this salt was more efficient as the great majority of Cu^{2+} ions, in this case, are chelated/adsorbed by such compounds.

For the subsequent studies, it was chosen the copper complexes with the highest Cu^{2+} content, for both copper sulfate and copper chloride salts, as determined by AAS.

Scanning electron microscopy (SEM) and energy-dispersive X-ray spectrometer (EDS) studies

The scanning electron micrograph of pure chitosan is shown in Fig. 1a. It exhibits smooth and compact morphology with some particle sizes. These surface morphology changes for Chitosan–Cu complex, Fig. 1b, due to the coordination of copper ion to the active sites of the biopolymer. The Schiff base presents irregular surface with agglomerates, as shown in Fig. 1c. The SEM images of CTB–Cu, Fig. 1d, revealed the presence of some crystals attributed to the presence of copper sulfate adsorbed on the polymer surface, confirmed by EDS analyses (Fig. 2b). The sample presented in the image was washed with distilled water at 50 °C three times in order to remove the copper sulfate adsorbed, however, the crystals were still observed in the image. The SEM images of CTB–Cu sample after being washed is shown in the inset of Fig. 1d. Figure 1e shows the surface morphology of NBC. It can also be seen a heterogeneous surface with small particle sizes accompanied with pores. The SEM image of NBC–Cu (Fig. 1f) also presented copper sulfate adsorbed on the surface. The morphology of the azo compound, Fig. 1g, presents roughness and pores in the surface. In the SEM image of Azo-NBC–Cu, the crystals of copper sulfate were

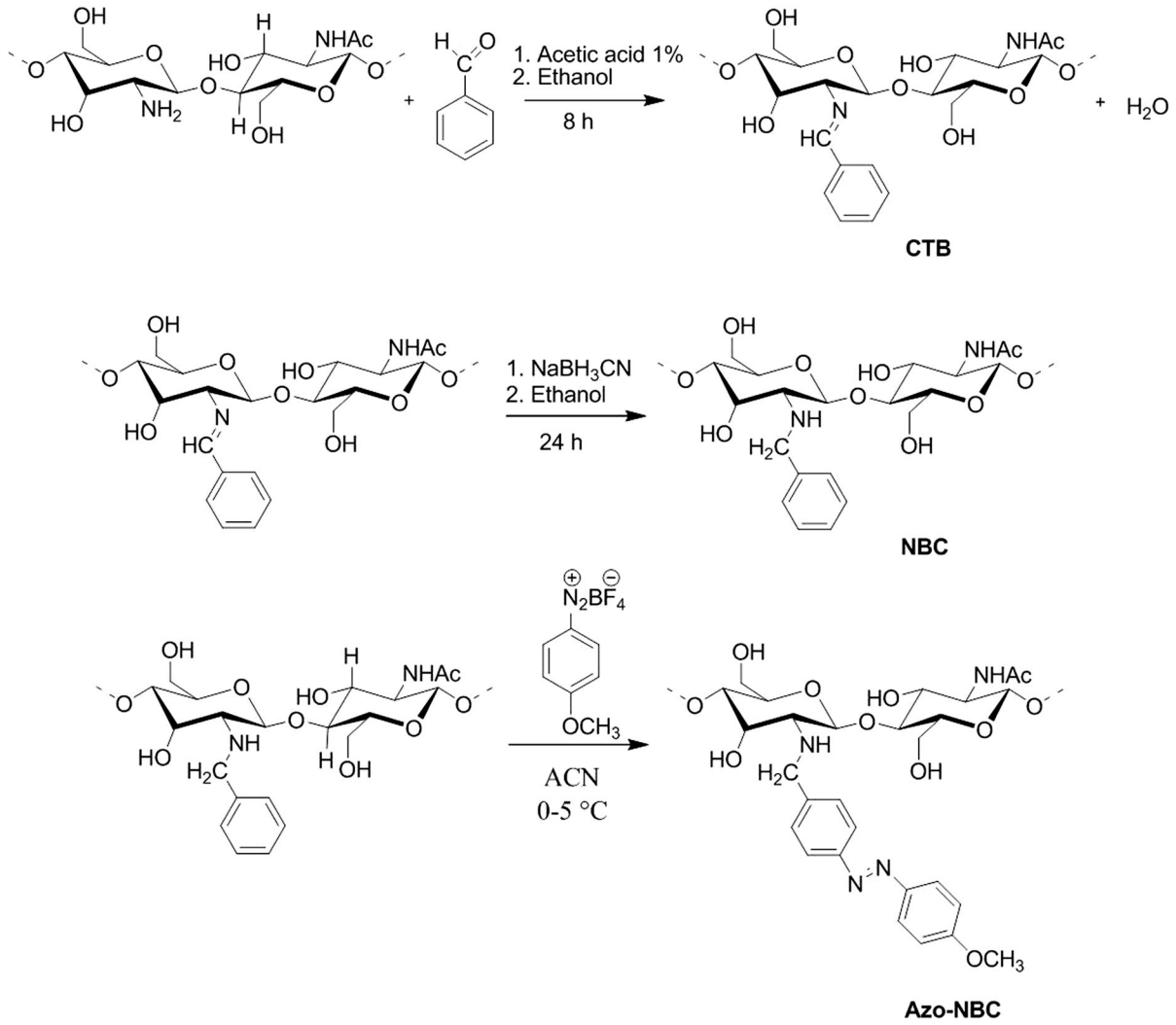

Scheme 1 Synthesis of chitosan compounds

Table 1 Concentration (mg/g) and percentage of Cu^{2+} ions chelated by chitosan and derivatives at different reaction times, 25 °C, using $CuSO_4 \cdot 5H_2O$ salt (0.01 mol/L)

Compound	30 min		24 h		36 h		48 h	
	mg/g	%	mg/g	%	mg/g	%	mg/g	%
Chitosan	73	45	**120**	**75**	120	75	120	75
CTB	24	15	73	45	**86**	**54**	86	54
NBC	8	5	23	14	**52**	**32**	40	25
Azo-NBC	5	3	15	10	**25**	**16**	25	16

Table 2 Concentration (mg/g) and percentage of Cu^{2+} ions chelated by chitosan and derivatives at 25 °C using $CuCl_2 \cdot 2H_2O$ salt (0.01 mol/L)

Compounds	Reaction time (h)	mg Cu^{2+}/g	% of Cu^{2+}
Chitosan	24	96	60
CTB	36	43	27
NBC	36	14	9
Azo-NBC	36	18	12

not observed due to the fact that this compound has the lowest capacity of chelating Cu(II), as displayed in Fig. 1h and confirmed by AAS studies.

The composition of Cu(II) complexes of chitosan and derivatives from $CuSO_4 \cdot 5H_2O$ salt was defined by energy-dispersive X-ray spectrometer (EDS) as shown

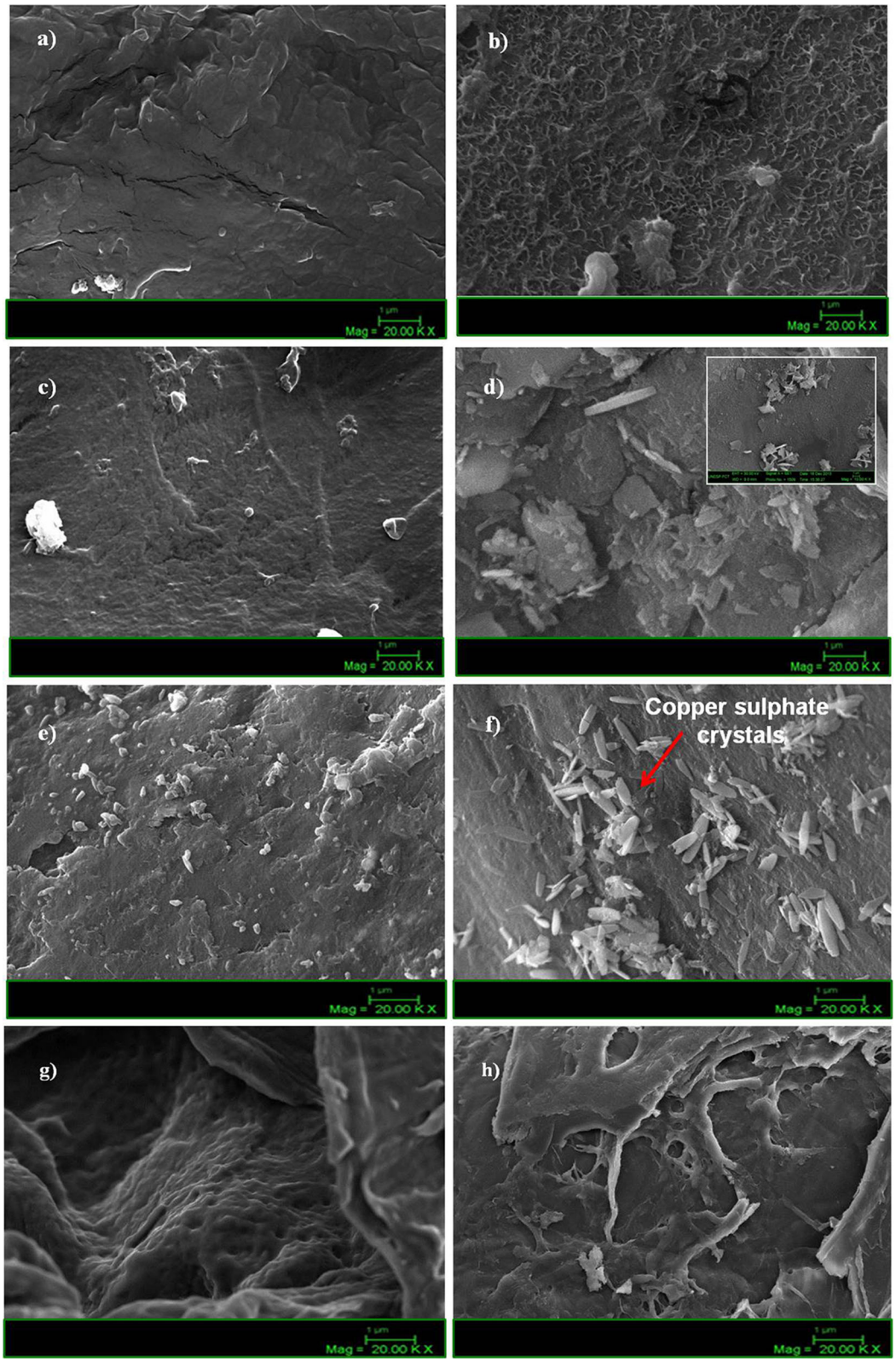
a)
b)
c)
d)
e)
f)
Copper sulphate crystals
g)
h)
Mag = 20.00 K X

◀**Fig. 1** SEM images of **a** Chitosan, **b** Chitosan–Cu, **c** CTB, **d** CTB–Cu with inset of the sample after being washed with distilled water, **e** NBC, **f** NBC–Cu, **g** Azo-NBC and **h** Azo-NBC–Cu, from $CuSO_4{\cdot}5H_2O$ salt. The *red arrow* shows the copper sulfate crystals. (Color figure online)

in Fig. 2. The results confirmed the existence of carbon, nitrogen and oxygen as well as copper and sulfur elements in all complexes. The presence of S corroborates with the SEM images in which were observed crystals on the surface of the complexes

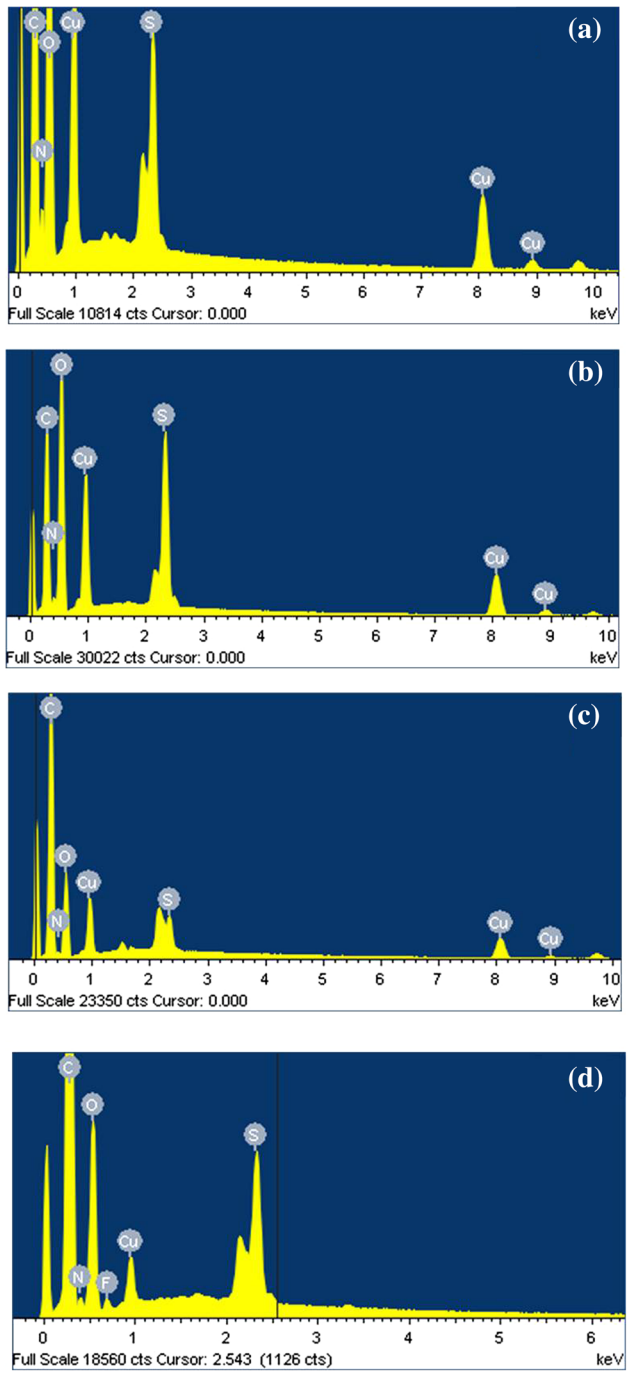

Fig. 2 EDS spectra of **a** Chitosan–Cu, **b** CTB–Cu, **c** NBC–Cu and **d** Azo-NBC–Cu, from $CuSO_4{\cdot}5H_2O$ salt

Chitosan-Cu

Element	Weight(%)
C K	39.26
N K	9.92
O K	45.63
S K	1.52
Cu K	3.67
Totals	100

CTB-Cu

Element	Weight(%)
C K	36.95
N K	8.96
O K	44.44
S K	3.68
Cu K	5.97
Totals	100

NBC-Cu

Element	Weight(%)
C K	57.45
N K	8.23
O K	28.83
S K	1.04
Cu K	4.45
Totals	100

Azo-NBC-Cu

Element	Weight(%)
C K	60.03
N K	10.14
O K	26.62
S K	1.45
Cu K	1.76
Totals	100

corresponding to copper sulfate. The results also indicated that Cu content is higher than S, which suggests that apart from copper sulfate adsorbed in the surface of the polymer, there are copper ions coordinated with the reactive sites of chitosan and derivatives. The EDS results for CTB–Cu after being washed with distilled water was the same for CTB–Cu before being washed, which indicates that this process did not remove the copper salt adsorbed by the polymer.

Moreover, it can be seen that the weight percent (%) of C element increases with the chemical modification of chitosan, as the weight percent (%) of N increases for Azo-NBC when compared to chitosan, CTB and NBC, confirming the formation of the azo derivative.

The SEM images of Chitosan–Cu, CTB–Cu, NBC–Cu and Azo-NBC–Cu, from $CuCl_2{\cdot}2H_2O$ salt, are displayed in Fig. 3a–d. The samples did not show any presence of crystals, which suggests that this salt was not adsorbed on the polymers surface. The agglomerates observed on NBC–Cu complex, Fig. 3c, were verified by EDS and the results indicated that they were not salt adsorbed by the compound, and were formed after chemical modification of chitosan. The EDS studies indicated a content of chlorine atom present in the complexes, Fig. 4. It might be due to the fact that this atom may take part in the coordination bond with the metal ion.

The reason why copper sulfate is adsorbed but not copper chloride can be associated to the stronger electric field in the divalent ion sulfate and the great distance of the hydration water from the ion center which can lead to a greater release of water molecules, resulting in an endothermic contribution for the salt adsorption on the polymer surface (Jiang et al. 2005).

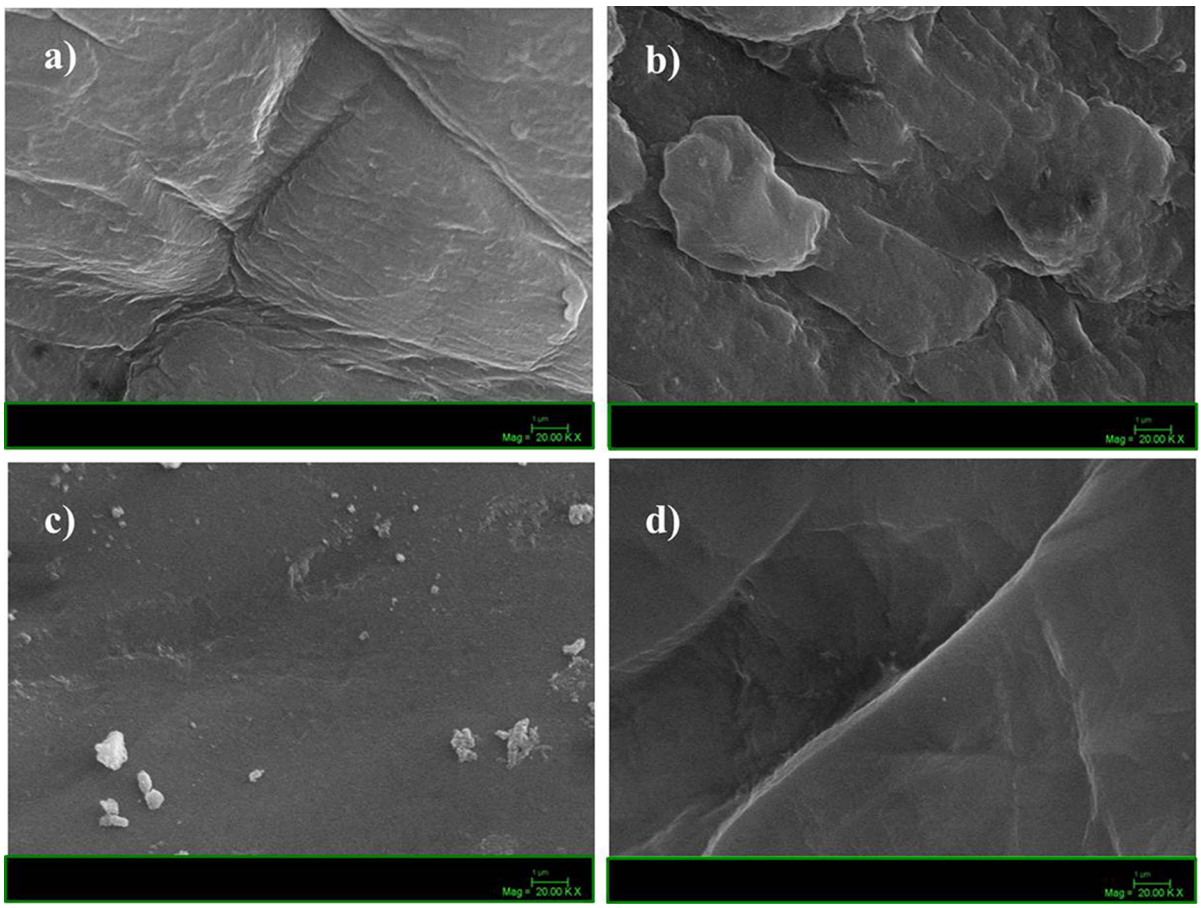

Fig. 3 SEM images of **a** Chitosan–Cu, **b** CTB–Cu, **c** NBC–Cu and **d** Azo-NBC–Cu, from $CuCl_2{\cdot}2H_2O$ salt

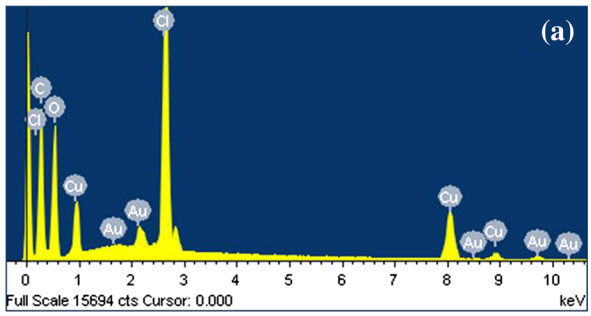

Chitosan-Cu

Elemento	% em peso
C K	50.76
O K	42.64
Cl K	2.57
Cu K	4.02
Total	100

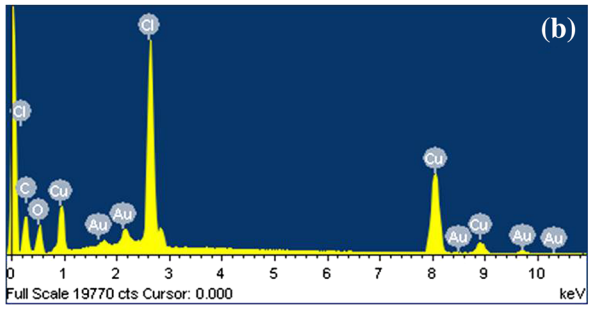

CTB-Cu

Elemento	% em peso
C K	52.50
O K	27.73
Cl K	8.60
Cu K	11.17
Totals	100

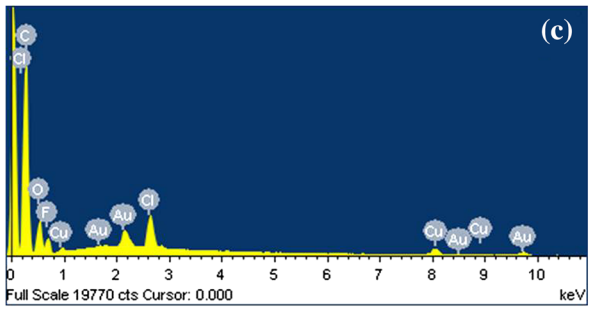

NBC-Cu

Elemento	% em peso
C K	67.03
O K	22.29
Cl K	0.54
Cu K	0.83
Total	100

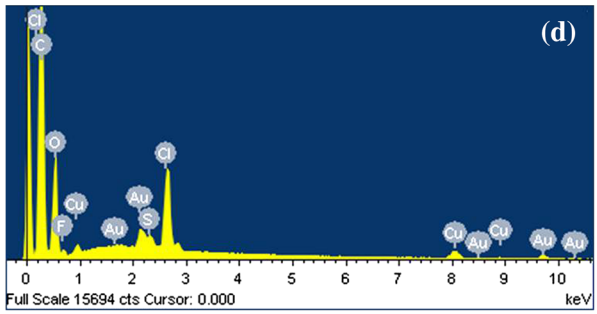

Azo-NBC-Cu

Elemento	% em peso
C K	64.94
O K	31.39
Cl K	0.34
Cu K	1.00
Totals	100

Fig. 4 EDS spectra of **a** Chitosan–Cu, **b** CTB–Cu, **c** NBC–Cu and **d** Azo-NBC–Cu, from $CuCl_2{\cdot}2H_2O$ salt

X-ray powder diffraction (XRD)

Figure 5 shows the X-ray diffraction patterns of chitosan, chitosan derivatives and the Cu^{2+} complexes from $CuSO_4{\cdot}5H_2O$ salt. The pattern of chitosan, Fig. 5a, showed the characteristic peaks at $2\theta = 9.5°$ and $2\theta = 20°$, which suggest the formation of inter- and intra-molecular hydrogen bonds in chitosan (Haas and Franz 2009). The XRD patterns of its copper complex showed a decrease in the intensity of the

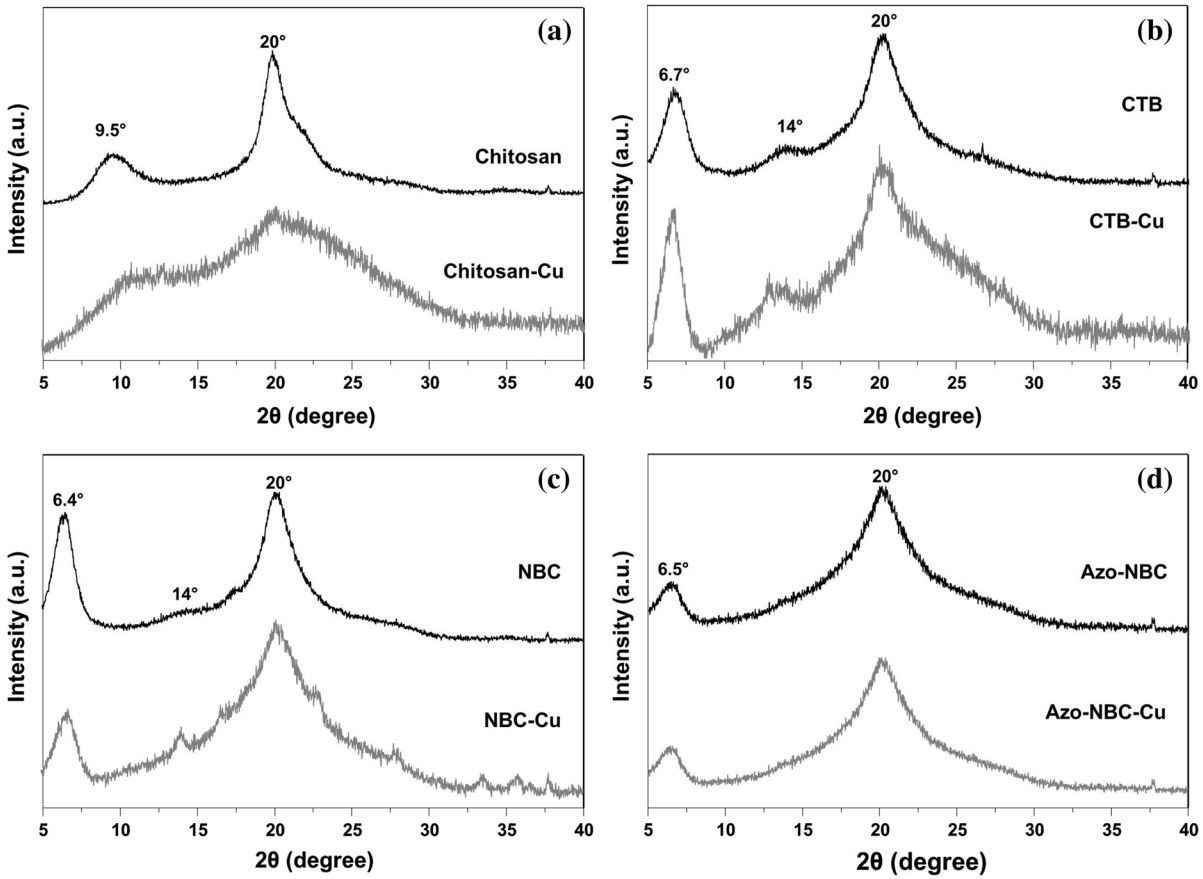

Fig. 5 X-ray diffraction patterns of **a** Chitosan and Chitosan–Cu, **b** CTB and CTB–Cu, **c** NBC and NBC–Cu and **d** Azo-NBC and Azo-NBC–Cu, from $CuSO_4{\cdot}5H_2O$ salt

peaks and they were more broadened than those observed for pure chitosan, indicating a low crystallinity of the complex (Anan et al. 2011).

In Fig. 5b, the XRD patterns of the Schiff base CTB showed a peak at $2\theta = 6.7°$ and a weak reflection at $2\theta = 14°$ due to the introduction of new groups in the side chain of chitosan (Li-xia et al. 2010). The peak at $2\theta = 20°$ is still observed for this compound. The XRD pattern of Schiff base Cu(II) complex, Fig. 5b, was appreciably different from CTB. It showed a remarkable decrease in crystallinity with a broad peak at $2\theta = 14°$ and 20°, due to the coordination with copper ions.

The X-ray diffraction patterns of NBC copper complex, Fig. 5c, showed a wider peak $2\theta = 20°$, evidencing a reduction in crystallinity as presented by the other complexes. Moreover, some smaller peaks that did not appear in the X-ray patterns of NBC are observed. It is characteristic of pure copper sulfate that is adsorbed on the polymer surface, as confirmed by SEM images.

X-ray diffraction patterns of Azo-NBC–Cu, Fig. 5d, did not show any significant difference when compared to the X-ray patterns of Azo-NBC due to the fact that this compound demonstrated lower capacity of metal chelation, as observed in AAS analysis.The crystallinity of the compounds was calculated using the following Eq. (1):

$$\text{Crystallinity index}\,(\%) = (I_{110} - I_{am}/I_{110}) \times 100 \quad (1)$$

where I_{110} is the maximum intensity at $\sim 20°$ and I_{am} is the intensity of amorphous diffraction at $\sim 10°$ (Focher et al. 1990).

Table 3 shows the calculated crystalline index values for all compounds. The crystallinity of chitosan derivatives decreased significantly, CTB 31 %, NBC

Table 3 Crystalline index of chitosan and derivatives and their respective Cu(II) complexes

Compound	Crystallinity index (%)
Chitosan	61
Chitosan–Cu	28
CTB	31
CTB–Cu	14
NBC	13
NBC–Cu	27
Azo-NBC	48
Azo-NBC–Cu	52

13 % and Azo-NBC 48 %, when compared to that of pure chitosan, 61 %. The change of crystallinity is mainly dependent on the presence of new groups bonded in the polymeric side chain and some other factors, such as spacial hindrance and hydrophobic force (Jeon and Höll 2003). The low crystallinity of chitosan derivatives indicates that they are more amorphous than the polymer. After coordinating with copper ion, chitosan and CTB have shown higher reduction of crystallinity noted by the less intense and wider diffraction peaks, being 28 and 14 %, respectively. This reduction was resulted from the deformation of strong hydrogen bonds (Yi et al. 2006) because copper ions may be coordinated with the nitrogen atoms and hydroxyl groups of the polymers. However, the crystallinity index values for NBC–Cu, 27 %, and Azo-NBC–Cu, 52 %, increased when compared to pure NBC and Azo-NBC. In the case of NBC–Cu, the increase in crystallinity is associated with the great amount of copper sulfate adsorbed on the derivative surface, as observed in the SEM image (Fig. 1f). This is also in agreement with the appearance of some peaks in the X-ray diffraction patterns of NBC–Cu, Fig. 5c. For Azo-NBC–Cu, the slight increase of crystallinity index can be due to the different coordination bond established by the azo-compound and the Cu^{2+} ions with participation of –N=N– groups. In addition, the lower concentration of copper ions coordinated with both compounds also generates a lower system disorder.

Raman spectroscopy

The Cu^{2+} complexes formed from $CuSO_4{\cdot}5H_2O$ salt was also studied by Raman spectroscopy. Figure 6 illustrates the Raman spectra of Chitosan and Chitosan–Cu. The characteristic peaks of chitosan are observed at 2936 and 2884 cm^{-1} attributed to the stretching vibrations of C–H groups, at 1661 cm^{-1} ascribed to amide I and at 1588 cm^{-1} due to the N–H deformation of amino groups. In addition, the peaks at 1456 and 1376 cm^{-1} are attributed to asymmetrical C–H bending of the CH_2 group, and the peak at 1256 cm^{-1} is assigned to O–H deformation vibration of the CH_2-OH group. The peaks at 1108 and 896 cm^{-1} are derived from the symmetric and asymmetric stretching vibrations of glycosidic bonds, respectively (Schrader 1995).

In the Raman spectrum of Chitosan–Cu, the signal at 1661 shifts to 1650 cm^{-1} and at 1588 to 1598 cm^{-1}. This result indicates the participation of these groups in the coordination bond with the metal. A new peak at 973 cm^{-1} is observed in the spectrum and attributed to stretching vibrations of O=S=O groups (Pye and Rudolph 2001; Rudolph et al. 2003; Hug 1997) due to the presence of $CuSO_4{\cdot}5H_2O$ salt adsorbed on the polymer surface. Bands related to metal and ligand vibrations, like Cu–O and Cu–N, could not be identified.

In comparison with chitosan spectrum, CTB Raman spectrum, Fig. 7, shows additional peaks at 1641 cm^{-1} due to C=N of imine group and at 3068, 1603 and 1000 cm^{-1} attributed to aromatic ring vibrations (Socrates 2001) The peak at 1583 cm^{-1} indicates that free $–NH_2$ groups are still present in the compound and were not chemically modified. The Raman spectrum of CTB–Cu presents the peak at 970 cm^{-1} due to stretching vibrations of O=S=O groups (Pye and Rudolph 2001; Rudolph et al. 2003; Hug 1997) because of the salt adsorbed on the polymer surface.

The Raman spectrum of NBC is presented in Fig. 8. The characteristic absorptions peaks are shown at 1585 cm^{-1} ascribed to the N–H deformation and at 3072, 1603 and 1000 cm^{-1} assigned to aromatic ring vibrations (Socrates 2001). In addition, the peak of the imine group at 1641 cm^{-1} disappears, which indicates the successful reduction of these groups. The Raman spectrum of NBC–Cu also presents the peak at 977 cm^{-1} due to stretching vibrations of O=S=O groups (Pye and Rudolph 2001; Rudolph et al. 2003; Hug 1997) because of the salt adsorbed on the derivative surface.

For the *N*-Azobenzyl compound, Azo-NBC, the Raman spectrum, Fig. 9, shows the characteristic peak

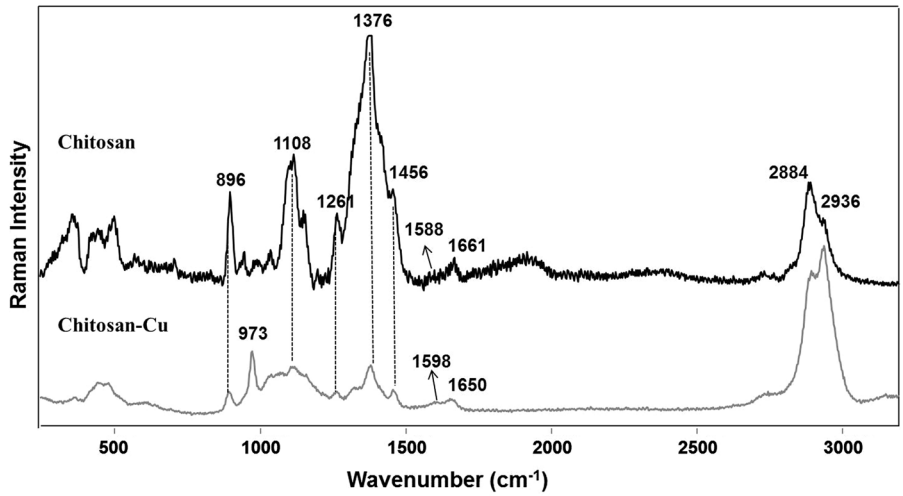

Fig. 6 Raman spectra of Chitosan and Chitosan–Cu

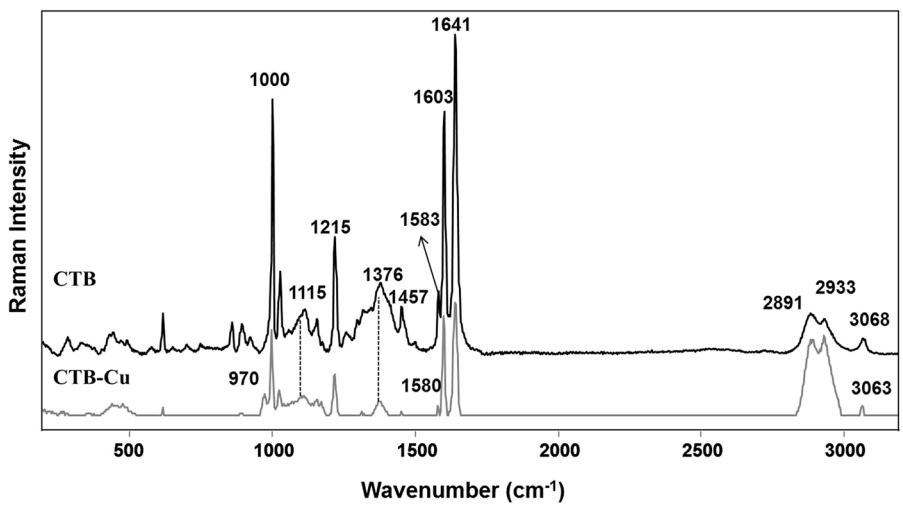

Fig. 7 Raman spectra of CTB and CTB–Cu

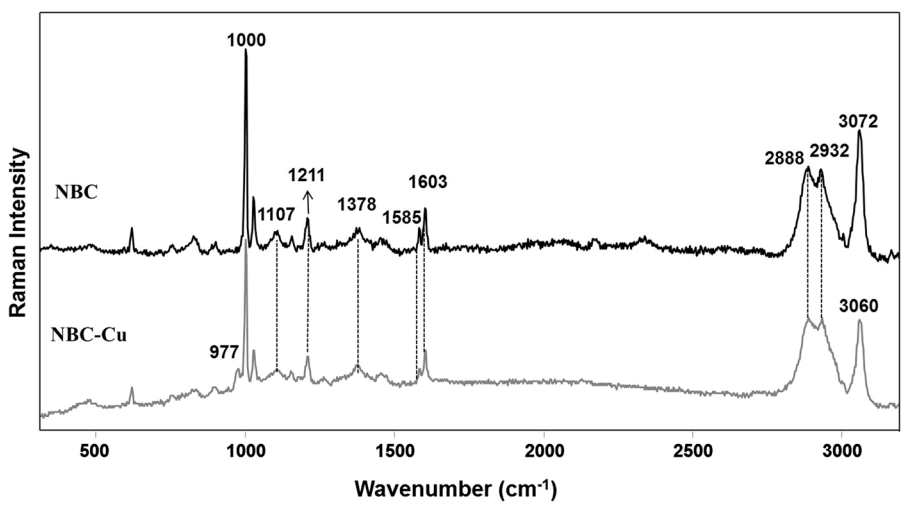

Fig. 8 Raman spectra of NBC and NBC–Cu

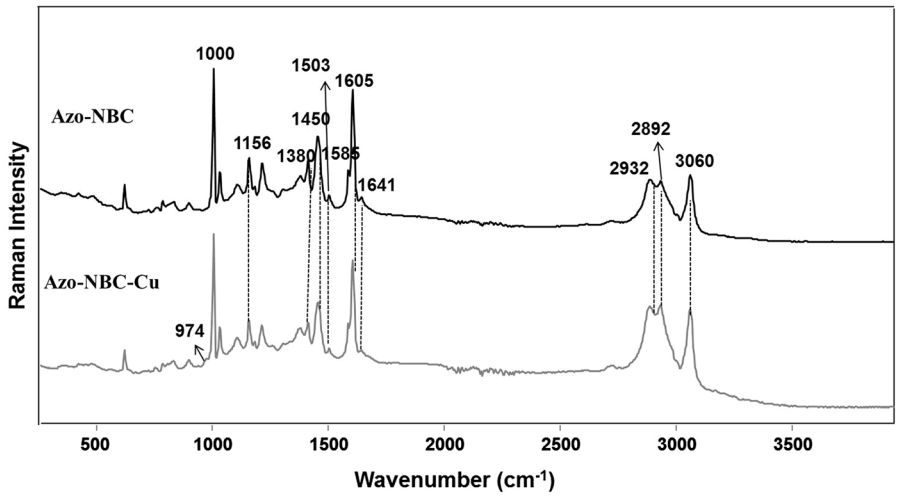

Fig. 9 Raman spectra of Azo-NBC and Azo-NBC-Cu

at 1503 cm^{-1} due to the N=N stretching vibration (Socrates 2001). In addition, the peaks at 3060, 1605 and 1000 cm^{-1} are assigned to aromatic ring vibrations. In the Raman spectrum of Azo-NBC–Cu, the stretching vibrations of O=S=O groups appear with a lower intensity at 974 cm^{-1} when compared to the other complexes. It might be due to lower capacity that this derivative presented to adsorb copper ions.

The presence of new peaks observed in the Raman spectra suggests the successful formation of the derivatives. Furthermore, the results of Cu^{2+} complexes corroborate with the information obtained by the SEM–EDS images which showed the presence of $CuSO_4{\cdot}5H_2O$ salt on the polymer surface.

Electron paramagnetic resonance (EPR)

The EPR spectra of chitosan and derivatives Cu(II) complexes, from copper sulfate salt, are represented in Fig. 10 and the values of $A_{//}$, $g_{//}$ and g⊥ are listed in Table 4. The results indicated the presence of copper ions in the polymers. The spectrum of Chitosan–Cu is typical of a monomeric copper center with resolved hyperfine structure in the so-called parallel direction, whose peak position and separation lead to the values of $g_{//}$ and $A_{//}$, respectively. The resolved parallel hyperfine structure vanishes upon complexation in CTB–Cu, NBC–Cu, and Azo-NBC–Cu, which hinders the determination of the respective values for those complexes. In these latter cases, only an average g-value can be determined directly from the spectra and those values are listed as g⊥ in Table 4. The g⊥ parameter for Chitosan–Cu was not calculated because the HFS was not resolved for the perpendicular orientation (Molochnikov et al. 2008).

One interesting feature observed in the spectra of CTB–Cu, NBC–Cu, and Azo-NBC–Cu is the complete change in lineshape when compared to Chitosan–Cu. All three spectra from the former complexes are very similar to each other and present only minor peaks with the parallel hyperfine structure visible. This suggests that the spectra seen in Fig. 10b–d contains two spectral components: one minor contribution, which would arise from copper centers similar to those found in Chitosan–Cu, and a major component coming from either dimeric or polymeric copper centers, where the copper center coupling would vanish the hyperfine interaction. This result corroborates with the large number of copper sulfate crystals observed in the SEM–EDS images.

Figure 11 shows the EPR spectra of chitosan and derivatives Cu(II) complexes, from copper chloride salt. The first observation that can be made is the presence of the well-resolved hyperfine structure as noticed above for Chitosan–Cu. This indicates that, for the complexes from copper chloride salt and unlike those from copper sulfate, the great majority of copper centers are monomeric and probably incorporated in the polymer. This result is in agreement with the images obtained by SEM–EDS analysis, in which great part of the copper retained from copper sulfate is in the salt adsorbed on the polymers surface.

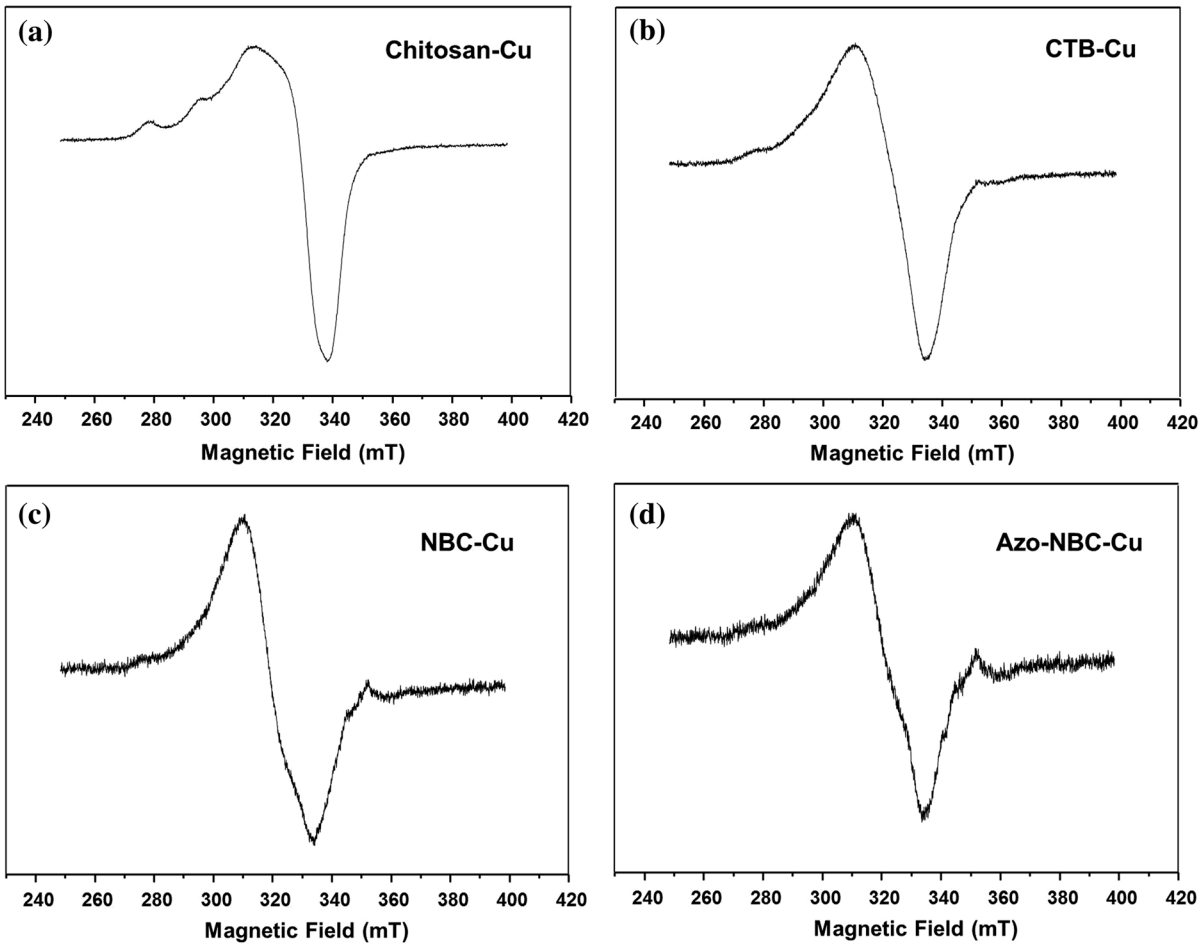

Fig. 10 EPR spectra of **a** Chitosan–Cu, **b** CTB–Cu, **c** NBC–Cu and **d** Azo-NBC–Cu, from $CuSO_4{\cdot}5H_2O$ salt

Table 4 EPR parameters of Cu^{2+} complexes from $CuSO_4{\cdot}5H_2O$ salt

Compounds	A‖ ($\times 10^4$ cm^{-1})	g‖	g⊥	g‖/A‖ (cm)
Chitosan–Cu	173.58	2.1947	–	126
CTB–Cu	–	–	2.06590	–
NBC–Cu	–	–	2.08643	–
Azo-NBC–Cu	–	–	2.08956	–

For the four complexes, $g_{//} > g\perp > 2.05$, which is suggestive of distorted tetragonal, square-pyramidal or square-planar geometry (Valdés and Triviño 2009).

Sakaguchi and Addison (1979) reported that the $g_{//}/A_{//}$ ratio can be used as a convenient empirical measure of tetrahedral distortion in Cu(II) complexes. This value ranges from 105 to 135 cm for square-planar structure, and this quotient increases on the introduction of tetrahedral distortion. Furthermore, tetrahedral distortion of a square-planar geometry is observed when $A_{//}$ reduces and $g_{//}$ increases. Thus, from the results in Table 5, the four compounds have a slightly tetrahedral distortion. The increase of $g_{//}$ values and decrease of $A_{//}$ values also show that the ligand field strength decreases in these compounds in the same order. Therefore, the complex Chitosan–Cu has a stronger ligand field than CTB–Cu, NBC–Cu and Azo-NBC–Cu.

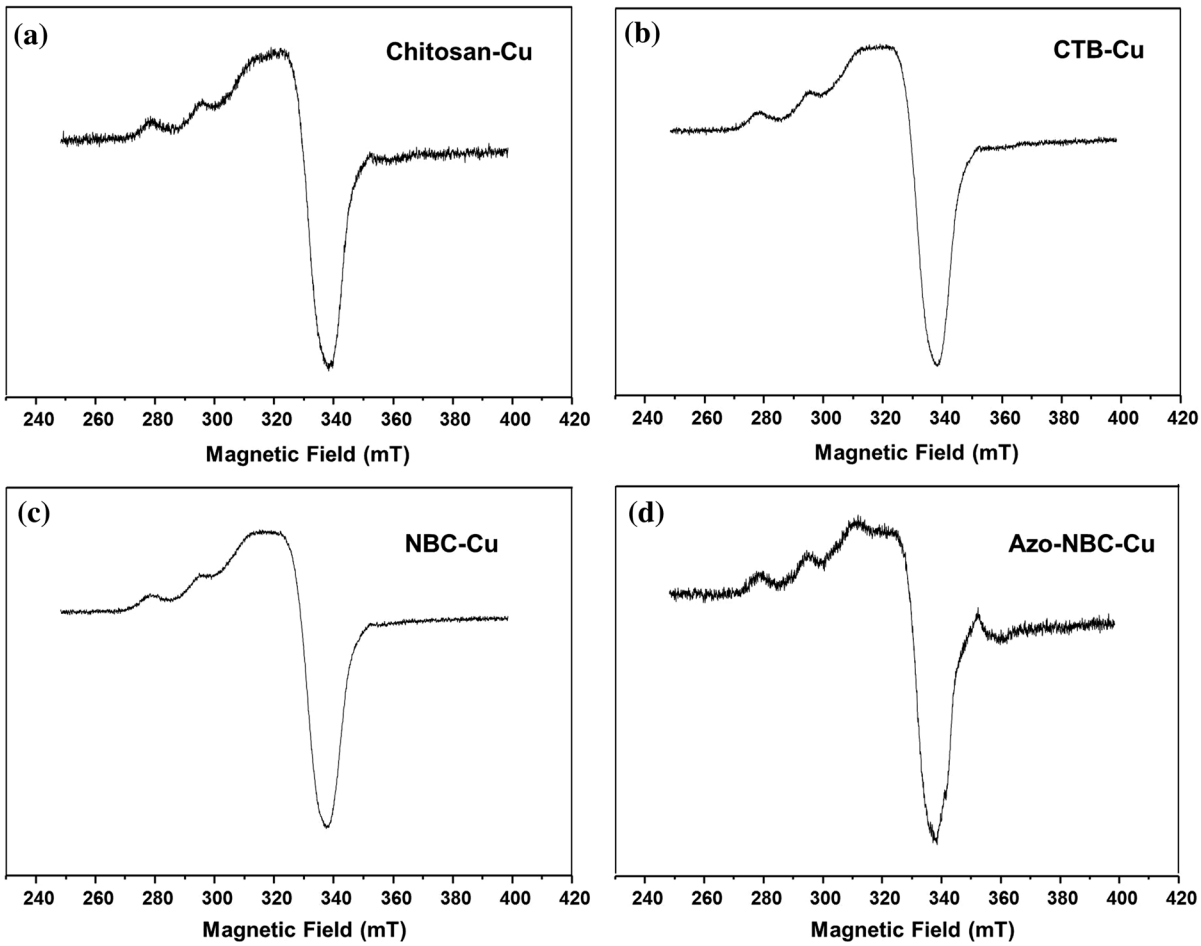

Fig. 11 EPR spectra of **a** Chitosan–Cu, **b** CTB–Cu, **c** NBC–Cu and **d** Azo-NBC–Cu, from $CuCl_4 \cdot 2H_2O$ salt

Table 5 EPR parameters of Cu^{2+} complexes from $CuCl_2 \cdot 2H_2O$ salt

Compounds	A∥ ($\times 10^4$ cm^{-1})	g∥	g⊥	g∥/A∥ (cm)
Chitosan–Cu	174.77	2.1637	–	124
CTB–Cu	173.58	2.1808	–	126
NBC–Cu	172.39	2.1825	–	126
Azo-NBC–Cu	169.99	2.1910	–	128

Conclusions

Chitosan compounds and their copper complexes have been synthesized and characterized by several techniques. The morphology studies by SEM–EDS exhibited copper sulfate adsorbed on the polymers surface, which indicates that part of the metal content determined by AAS is in the salt adsorbed and might influence in the use of the materials for further application studies, for instance, it can promote variation on reproducibility of catalysis experiments or compromise their biological activity. The presence of the salt was confirmed by Raman spectroscopy. X-ray diffraction patterns showed that the chemical modification of chitosan and formation of complexes resulted in the decrease of crystallinity. This decrease is mainly attributed to the spatial hindrance and hydrophobic forces in the aromatic substituent groups and to the deformation of strong hydrogen bonds when Cu^{2+} is coordinated to the compounds. EPR spectra of the complexes from copper chloride salt showed that the great majority of copper centers are monomeric and probably incorporated in the polymer, unlike those

from copper sulfate. EPR parameters also suggested that the Cu^{2+} complexes present a square-planar geometry.

Acknowledgments The authors gratefully thank Fundação de Apoio a Pesquisa do Estado de São Paulo (FAPESP), 2012/13901-3, Programa de Pós-graduação em Ciência e Tecnologia de Materiais (POSMAT) and Coordenação de Aperfeiçoamento de Pessoal de Nível Superior (CAPES) for financial support and post-graduation fellowship. The authors thank Leonardo Negri Furini (UNESP—Presidente Prudente, SP) and Dr. Jose Vicente García Ramos (CSIC—Madrid, Spain) for Raman Spectroscopy analyses.

References

Adlim M, Bakar A, Liew KY, Ismail J (2004) Synthesis of chitosan-stabilized platinum and palladium nanoparticles and their hydrogenation activity. J Mol Catal A Chem 212:141–149

Anan NA, Hassan SM, Saad EM, Butler IS, Mostafa IS (2011) Preparation, characterization and pH-metric measurements of 4-hydroxysalicylidenechitosan Schiff-base complexes of Fe(III), Co(II), Ni(II), Cu(II), Zn(II), Ru(III), Rh(III), Pd(II) and Au(III). Carbohydr Res 346:775–793

Anastas PT, Kirchhoff MM, Williamson TC (2001) Catalysis as a foundational pillar of green chemistry. Appl Catal A Gen 221:3–13

Bassi R, Prasher SO, Simpson BK (2000) Removal of selected metal ions from aqueous solutions using chitosan flakes. Sep Sci Technol 35:547–560

Borch RF, Bernstei MD, Durst HD (1971) Cyanohydridoborate anion as a selective reducing agent. J Am Chem Soc 93:2897–2904

Calo V, Nacci A, Monopoli A, Fornaro A, Sabbatini L, Cioffi N, Ditaranto N (2004) Heck reaction catalyzed by nanosized palladium on chitosan in ionic liquids. Organometallics 23:5154–5158

Cárdenas G, Taboada E, Bravo A, Miranda SP (2003) SEM–EDX studies of chitosan derivatives–metal adducts. J Chil Chem Soc 48(4):49–53

Chassary P, Vincen T, Guibal E (2004) Metal anion sorption on chitosan and derivative materials: a strategy for polymer modification and optimum use. React Funct Polym 60:137–149

Das SD, Mukherjee S, Lopes LMF, Ilharco LM, Ferraria AM, Rego AMB, Pombeiro AJL (2014) Synthesis, characterization and heterogeneous catalytic application of copper integrated mesoporous matrices. Dalton Trans 43:3215–3226

Delben F, Stefancich S, Muzzarelli RAA (1992) Chelating ability and enzymatic hydrolysis of water-soluble chitosans. Carbohydr Polym 19:17–23

Dobetti L, Delben F (1992) Binding of metal cations by *N*-carboxymethyl chitosans in water. Carbohydr Polym 18:273–282

Domard A (1987) pH and c.d. measurements on a fully deacetylated chitosan: application to Cu^{II}–polymer interactions. Int J Biol Macromol 9:98–104

Dulcevscaia GM et al (2013) New copper(II) complexes with isoconazole: synthesis, structures and biological properties. Polyhedron 52:106–114

Facchin G, Kremer E, Barrio DA, Etcheverry SB, Costa-Filho AJ, Torre MH (2009) Interaction of Cu–dipeptide complexes with Calf Thymus DNA and antiproliferative activity of [Cu(ala-phe)] in osteosarcoma-derived cells. Polyhedron 28:2329–2334

Focher B, Beltrame PL, Naggi A, Torri G (1990) Alkaline N-deacetylation of chitin enhanced by flash treatments. Reaction kinetics and structure modification. Carbohydr Polym 12:405–418

Genin JM, Biles C, Keiser JB, Poppe SM, Swaney SM, Tarapley WG, Romero DL, Yagi Y (2000) Novel 1,5-diphenylpyrazole nonnucleoside HIV-1 reverse transcriptase inhibitors with enhanced activity versus the delavirdine-resistant P236L mutant: lead identification and SAR of 3- and 4-substituted derivatives. J Med Chem 43:1034–1040

Giovagnini L, Sitran S, Caparrotta L, Corsini M, Rosani C, Zanello P, Dou QP, Fregona D (2008) Chemical and biological profiles of novel copper(II) complexes containing S-donor ligands for the treatment of cancer. Inorg Chem 47(14):2

Guibal E (2004) Interactions of metal ions with chitosan-based sorbents: a review. Sep Purif Technol 38:43–74

Guibal E (2005) Heterogeneous catalysis on chitosan-based materials: a review. Prog Polym Sci 30:71–109

Haas LK, Franz JK (2009) Application of metal coordination chemistry to explore and manipulate cell biology. Chem Rev 109:4921–4960

Huang C, Chuang YC, Liou MR (1996) Adsorption of Cu(II) and Ni(II) by pelletized biopolymer. J Hazard Mater 45:265–277

Hug SJ (1997) In situ fourier transform infrared measurements of sulfate adsorption on hematite in aqueous solutions. J Colloid Interface Sci 188:415–422

Iakovidis I, Delimaris I, Piperakis SM (2011) Copper and its complexes in medicine: a biochemical approach. Mol Biol Int

Jeon C, Höll WH (2003) Chemical modification of chitosan and equilibrium study for mercury ion removal. Water Res 37:4770–4780

Jiang N, Li P, Wang Y, Wang J, Haike Y, Thomas RK (2005) Aggregation behavior of hexadecyltrimethylammonium surfactants with various counterions in aqueous solution. J Colloid Interface Sci 286:755–760

Jiao TF, Zhou J, Zhou JX, Gao LH, Xing YY, Li XH (2001) Synthesis and characterization of chiosan-based Schiff base compounds with aromatic substituent groups. Iran Polym J 20:123–136

Katwal R, Kaur H, Kapur BK (2013) Applications of copper – Schiff's base complexes: a review. Sci Rev Chem Commun 3:1–15

Li-xia W, Zi-wei W, Guo-song W, Xiao-dong L, Jian-guo R (2010) Catalytic performance of chitosan-Schiff base supported Pd/Co bimetallic catalyst for acrylamide with phenyl halide. Polym Adv Technol 21:244–249

Molochnikov LS, Pesto AV, Zabolotskaya EV, Yatluk YG (2008) Solid-state structure of copper complexes of *N*-(2-carboxyethyl)chitosan. J Appl Spectrosc 75:648–652

Ogawa K, Oka K (1993) X-ray study of chitosan–transition metal complexes. Chem Mater 5:726–728

Ogawa K, Oka K, Miyanish T, Hirano S (1984) X-ray diffraction study of chitosan-metal complexes, in Chitin, Chitosan and Related Enzimes. Academic Press, Orlando, pp 327–345

Pereira FS, da Silva Agostini DL, Job AE, González ERP (2013) Thermal studies of chitin–chitosan derivatives. J Therm Anal Calorim 114:321–327

Pereira FS, Nascimento HDL, Magalhães A, Peter MG, Bataglion GA, Eberlin MN, González ERP (2014) ESI(+)-MS and GC-MS study of the hydrolysis of *N*-Azobenzyl derivatives of chitosan. Molecules 19:17604–17618

Pye CC, Rudolph WW (2001) An ab initio and Raman investigation of sulfate ion hydration. J Phys Chem A 105:905–912

Rhazi M, Desbrières J, Tolaimate A, Rinaudo M, Vottero P, Alagui A (2002) Contribution to the study of complexation of copper by chitosan and oligomers. Polymer 43:1267–1276

Rodrigues CA, Laranjeira MCM, de Favere VT, Sadler E (1998) Interaction of Cu(II) on *N*-(2-pyridylmethyl) and *N*-(4-pyridylmethyl) chitosan. Polymer 39:5121–5126

Rudolph WW, Irmer G, Hefter GT (2003) Raman spectroscopic investigation of speciation in $MgSO_4$(aq). Phys Chem Chem Phys 5:5253–5261

Sajomsang W, Tantayanon S, Tangpasuthadol V, Thatte M, Daly WH (2006) Synthesis and characterization of *N*-benzyl chitosan derivatives. Polym Prepr 47:294–295

Sakaguchi U, Addison AW (1979) Spectroscopic and redox studies of some copper (II) complexes with biomimetic donor atoms: implications for protein copper centres. J Chem Soc Dalton Trans 4:600–608

Schlick SH (1986) Binding sites of Cu^{2+} in chitin and chitosan. An electron spin resonance study. Macromolecules 19:192–195

Schrader B (1995) Infrared and Raman spectroscopy, methods and applications. VCH Publishers, Inc., New York

Socrates G (2001) Infrared and Raman characteristic group frequencies, 3rd edn. Wiley-VCH, England

Suslick KS, Reinert TJ (1985) The synthetic analogs of O2-binding heme proteins. Novel 1,5-diphenylpyrazole non-nucleoside HIV-1 reverse transcriptase inhibitors with enhanced activity versus the delavirdine-resistant P236L Mutant: lead Identification and SAR of 3- and 4-substituted derivatives. J Chem Educ 62:974–983

Torre MH, Gambino D, Araujo J, Cerecetto H, González M, Lavaggi ML, Azqueta A, Cerain AL, Vega AM, Abram U, Costa-Filho AJ (2005) Novel Cu(II) quinoxaline N^1, N^4-dioxide as selective hypoxic cytotoxins. Eur J Med Chem 40:473–480

Urquiola C, Gambino D, Cabrera M, Lavaggi ML, Cerecetto H, González M, Cerain AL, Monge A, Costa-Filho AJ, Torre MH (2008) New copper-based complexes with quinoxaline N^1, N^4-dioxide derivatives, potential antitumoral agents. J Inorg Biochem 102:119–126

Valdés ET, Triviño GC (2009) Chitosan metal complexes and chitosan–Cu ESR studies. J Chil Chem Soc 54(1):1–5

Wang XH, Du YM, Fan LH, Huang RH, Zhang LN, Hu L (2005) Chitosan–metal complexes as antimicrobial agent: synthesis, characterization and structure–activity study. Polym Bull 55:105–113

Wang H, Bao C, Li F, Kong X, Xu J (2010) Preparation and application of 4-amino-4′-nitro azobenzene modified chitosan as a selective adsorbent for the determination of Au(III) and Pd(II). Microchim Acta 168:99–105

Wang H, Li C, Bao C, Liu L, Liu X (2011) Adsorption and determination of Pd(II) and Pt(IV) onto 3′-nitro-4-amino azobenzene modified chitosan. J Chem Eng Data 56:4203–4207

Yi Y, Wang Y, Ye F (2006) Synthesis and properties of diethylene triamine derivative of chitosan. Colloids Surf A 277:69–74

Zheng Y, Yi Y, Qi Y, Wang Y, Zang W, Du M (2006) Preparation of chitosan–copper complexes and their antitumor activity. Bioorg Med Chem Lett 16:4127–4129